

Generation of a Peroxynitrato Metal Complex from Nitrogen Dioxide and Coordinated Superoxide

Oleg Pestovsky and Andreja Bakac*

Ames Laboratory and Chemistry Department, Iowa State University, Ames, Iowa 50011

Received December 31, 2002

The reaction between photogenerated NO_2 radicals and a superoxochromium(III) complex, $\text{Cr}_{\text{aq}}\text{OO}^{2+}$, occurs with rate constants $k_{\text{Cr}^{20}} = (2.8 \pm 0.2) \times 10^8 \text{ M}^{-1} \text{ s}^{-1}$ (20 vol % acetonitrile in water) and $k_{\text{Cr}^{40}} = (2.6 \pm 0.5) \times 10^8 \text{ M}^{-1} \text{ s}^{-1}$ (40 vol % acetonitrile) in aerated acidic solutions and ambient temperature. The product was deduced to be a peroxynitrato complex, $\text{Cr}_{\text{aq}}\text{OONO}_2^{2+}$, which undergoes homolytic cleavage of an N–O bond to return to the starting materials, the rate constants in the two solvent mixtures being $k_{\text{H}^{20}} = 172 \pm 4 \text{ s}^{-1}$ and $k_{\text{H}^{40}} = 197 \pm 7 \text{ s}^{-1}$. NO_2 reacts rapidly with 10-methyl-9,10-dihydroacridine, $k_{\text{A}^{20}} = 2.2 \times 10^7 \text{ M}^{-1} \text{ s}^{-1}$, $k_{\text{A}^{40}} = (9.4 \pm 0.2) \times 10^6 \text{ M}^{-1} \text{ s}^{-1}$, and with *N,N,N',N'*-tetramethylphenylenediamine, $k_{\text{T}^{40}} = (1.84 \pm 0.03) \times 10^8 \text{ M}^{-1} \text{ s}^{-1}$.

Introduction

The recent surge in interest in the chemistry of nitrogen oxides has been triggered by several findings showing that these small inorganic molecules play key roles in such diverse processes as the generation of tropospheric ozone and acid rain, physiological signaling, blood pressure control, immune response, aging, and disease.^{1–3} As a result, a large body of work on nitrogen monoxide, NO , has been published.^{3–10} Similarly, species derived from NO , such as peroxynitrite, OONO^- , and its conjugate acid, HOONO ($\text{p}K_{\text{a}} = 6.8$),¹¹ also have received much attention^{12–20} owing

to their oxidizing and nitrating power and a potential role in harmful biological processes. Nitrogen dioxide, on the other hand, has been explored much less,²¹ even though it, too, is a strong oxidant and nitrating species and may well be responsible^{22,23} for some of the damage attributed to peroxynitrite from which it is (at least, formally) derived by homolytic cleavage of the peroxy bond. Probably the most common source of NO_2 in an aerobic organism is the reaction of oxyglobins with nitric oxide,²⁴ eq 1 (where L represents the ligand(s) and protein environment around the iron).



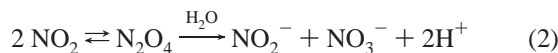
One of the reasons for the limited literature data on the reactivity of NO_2 in general, and in complex systems in

* To whom correspondence should be addressed. E-mail: Bakac@ameslab.gov.

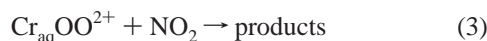
- (1) Lerdau, M. T.; Munger, J. W.; Jacob, D. J. *Science* **2000**, *289*, 2291–2293.
- (2) Richter-Addo, G. B.; Legzdins, P.; Burstyn, J. *Chem. Rev.* **2002**, *102*, 857–859.
- (3) *Nitric Oxide. Biology and Pathobiology*; Ignarro, L. J., Ed. Academic: San Diego, CA, 2000.
- (4) Lancaster, J. R., Jr. *Am. Sci.* **1992**, *80*, 248–259.
- (5) Garry, D. J.; Ordway, G. A.; Lorenz, J. N.; Radford, N. B.; Chin, E. R.; Grange, R. W.; Bassel-Duby, R.; Williams, R. S. *Nature* **1998**, *395*, 905–908.
- (6) Goldstein, S.; Czapski, G. *J. Am. Chem. Soc.* **1995**, *117*, 12078–12084.
- (7) Wade, R. S.; Castro, C. E. *Chem. Res. Toxicol.* **1996**, *9*, 1382–1390.
- (8) Ford, P. C.; Lorkovic, I. M. *Chem. Rev.* **2002**, *102*, 993–1018.
- (9) Moller, J. K. S.; Skibsted, L. H. *Chem. Rev.* **2002**, *102*, 1167–1178.
- (10) Wang, P. G.; Xian, M.; Tang, X.; Wu, X.; Wen, Z.; Cai, T.; Janczuk, A. *J. Chem. Rev.* **2002**, *102*, 1091–1134.
- (11) Koppenol, W. H.; Moreno, J. J.; Pryor, W. A.; Ischiropoulos, H.; Beckman, J. S. *Chem. Res. Toxicol.* **1992**, *5*, 834–842.
- (12) Pryor, W. A.; Squadrito, G. L. *Am. J. Physiol.* **1995**, *268*, L699–L722.
- (13) Squadrito, G. L.; Pryor, W. A. *Free Radical Biol. Med.* **1998**, *25*, 392–403.

- (14) Beckman, J. S.; Koppenol, W. H. *Am. J. Physiol.* **1996**, *271*, C1424–C1437.
- (15) Hodges, G. R.; Ingold, K. U. *J. Am. Chem. Soc.* **1999**, *121*, 10695–10701.
- (16) Stern, M. K.; Jensen, M. P.; Kramer, K. *J. Am. Chem. Soc.* **1996**, *118*, 8735–8736.
- (17) Marla, S. S.; Lee, J.; Groves, J. T. *Proc. Natl. Acad. Sci. U.S.A.* **1997**, *94*, 14243–14248.
- (18) Shimanovich, R.; Groves, J. T. *Arch. Biochem. Biophys.* **2001**, *387*, 307–317.
- (19) Herold, S.; Matsui, T.; Watanabe, Y. *J. Am. Chem. Soc.* **2001**, *123*, 4085–4086.
- (20) Eich, R. F.; Li, T.; Lemon, D. D.; Doherty, D. H.; Curry, S. R.; Aitken, J. F.; Mathews, A. J.; Johnson, K. A.; Smith, R. D.; Phillips, G. N., Jr.; Olson, J. S. *Biochemistry* **1996**, *35*, 6976–6983.
- (21) Neta, P.; Huie, R. E.; Ross, A. B. *J. Phys. Chem. Ref. Data* **1988**, *17*, 1027–1284.
- (22) Espey, M. G.; Xavier, S.; Thomas, D. D.; Miranda, K. M.; Wink, D. A. *Proc. Natl. Acad. Sci. U.S.A.* **2002**, *99*, 3481–3486.
- (23) Pfeiffer, S.; Lass, A.; Schmidt, K.; Mayer, B. *FASEB J.* **2001**, *15*, 2355–2364.
- (24) Doyle, M. P.; Hoekstra, J. W. *J. Inorg. Biochem.* **1981**, *14*, 351–358.

particular, is the difficulty in observing clearly the chemistry of NO₂ in the presence of its typical, reactive precursors, free or bound peroxytrite. Also, unlike NO and peroxytrite, NO₂ is a short-lived species which rapidly dimerizes and disproportionates,²⁵ eq 2. Direct kinetic measurements with chemically or photochemically generated NO₂ thus suffer from the same difficulties encountered in studies of all the transient radicals; i.e., the reactions with desired substrates have to be fast to be observable above the background radical self-reactions. Because of the weak UV–vis spectrum of NO₂, it is also necessary for the reaction partners to provide the needed absorbance change for the reaction. Alternatively, a kinetic probe is required.



Here we report our observations on the reaction of NO₂ with a superoxochromium(III) complex, Cr_{aq}OO²⁺, eq 3. This reaction is involved in Cr_{aq}OO²⁺-catalyzed oxidation of alcohols by molecular oxygen in the presence of nitrous acid.²⁶



Earlier, we explored briefly the kinetics for the initial interaction in acidic aqueous solution.²⁷ Now we present mechanistic details, product analysis, and additional kinetic data in mixed acetonitrile/water solvents. To the best of our knowledge, this is the first documented example of a reaction between NO₂ and a superoxometal complex despite the great likelihood that encounters between NO₂ and oxyglobins (and possibly other metal–dioxygen complexes) take place frequently in biological environments. The oxidation of oxy-hemoglobin by NO₂ has been invoked as a step in autocatalytic oxidation of hemoglobin by nitrite,²⁸ but that chemistry has not been confirmed. In another paper, oxymyoglobin was reported to react with NO₂ only indirectly after the hydrolysis to nitrite.⁷

The following abbreviations are used throughout the paper: TMPD = *N,N,N',N'*-tetramethylphenylenediamine, NADH = nicotinamide adenine dinucleotide, AN = acetonitrile, AcrH₂ = 10-methyl-9,10-dihydroacridine.

Experimental Section

Materials. Reagent grade perchloric acid, zinc metal, mercury(II) chloride, methanol, acetonitrile, sodium acetate, and *N,N,N',N'*-tetramethylphenylenediamine (TMPD) were used as received. Nitrogen dioxide gas was purchased from Aldrich. Pentaammine-nitrocobalt(III) triflate and chromium(III) perchlorate were available from our previous studies.²⁹ In-house deionized water was further purified by passage through a Millipore Milli-Q system.

10-Methyl-9,10-dihydroacridine (AcrH₂) was synthesized according to a literature procedure.³⁰ Chart 1 shows structural formulas of different forms of dihydroacridine observed in this study.

(25) Stedman, G. *Adv. Inorg. Chem. Radiochem.* **1979**, *22*, 113–170.

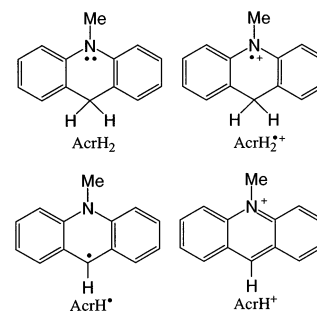
(26) Pestovsky, O.; Bakac, A. Manuscript in preparation.

(27) Nemes, A.; Pestovsky, O.; Bakac, A. *J. Am. Chem. Soc.* **2002**, *124*, 421–427.

(28) Lissi, E. *Free Radical Biol. Med.* **1998**, *24*, 1535–1536.

(29) Bakac, A. *J. Am. Chem. Soc.* **2000**, *122*, 1092–1097.

Chart 1



Solutions of Cr_{aq}²⁺ were prepared by the reduction of the respective 3+ ion with zinc amalgam under anaerobic conditions. Stock solutions of 0.15–0.3 mM Cr_{aq}OO²⁺ were prepared by injecting Cr_{aq}²⁺ into ice-cold, oxygen-saturated 0.1 M HClO₄ containing 0.044 M methanol. Such solutions were standardized spectrophotometrically ($\epsilon_{293} = 3.0 \times 10^3 \text{ M}^{-1} \text{ cm}^{-1}$)³¹ and used within 1 h of preparation.

Concentrations of various acridine species in 20% aqueous acetonitrile (AN) were determined spectrophotometrically:³² AcrH₂, $\epsilon_{285} = 1.32 \times 10^4 \text{ M}^{-1} \text{ cm}^{-1}$; AcrH⁺, $\epsilon_{417} = 3.94 \times 10^3 \text{ M}^{-1} \text{ cm}^{-1}$; and AcrH₂^{•+}, $\epsilon_{640} = 6.44 \times 10^3 \text{ M}^{-1} \text{ cm}^{-1}$. The molar absorptivity at 565 nm of the TMPD radical, generated by oxidation of TMPD with Ce(IV) in 40% AN buffered with 0.05 M CH₃COOH/0.05 M CH₃COONa, was measured to be $\epsilon_{565} = 1.29 \times 10^4 \text{ M}^{-1} \text{ cm}^{-1}$. Nitrate and nitrite ion analyses were carried out as described previously.³³ The acidity constant of TMPDH⁺ in 40% AN was determined from the pH of a solution containing 4.61 mM TMPD and 2.32 mM HClO₄, pK_a = 5.79. pH measurements were carried out with the use of an ATC pH electrode (Corning).

Kinetics. Most kinetic experiments were carried out at [H⁺] = 0.10 M and room temperature in aerated solutions, unless stated otherwise. UV–vis spectra were recorded by use of a Shimadzu 3101 PC spectrophotometer. Laser flash photolysis experiments utilized an Applied Photophysics Nd:YAG laser system ($\lambda_{\text{exc}} = 355 \text{ nm}$) and a Phase-R model DL-1100 dye laser ($\lambda_{\text{exc}} = 426 \text{ nm}$), which were described elsewhere.^{34,35} To minimize sample photolysis by the analyzing light at longer times in the dye laser system, a 399-nm cutoff filter was used.

Stopped-flow measurements utilized an Applied Photophysics DX-17MV stopped-flow instrument. Nonlinear least-squares fittings were performed with the use of Kaleidagraph 3.0 for PC software. Consecutive biphasic treatment of kinetic traces utilized the shown integrated rate law, where k_1 and k_2 are first-order rate constants for the two reaction stages, [A]₀ is the initial concentration of the reactant A, and ϵ_{int} is the molar absorptivity of the observable intermediate.³⁶

$$\text{Abs} = \frac{k_1[A]_0\epsilon_{\text{int}}}{k_2 - k_1} [\exp(-k_1t) - \exp(-k_2t)]$$

(30) Karrer, P.; Szabo, L.; Krishna, H. J. V.; Schwyzer, R. *Helv. Chim. Acta* **1950**, *33*, 294–300.

(31) Ilan, Y. A.; Czapski, G.; Ardon, M. *Isr. J. Chem.* **1975**, *13*, 15–21.

(32) Pestovsky, O.; Bakac, A.; Espenson, J. H. *Inorg. Chem.* **1998**, *37*, 1616–1622.

(33) Pestovsky, O.; Bakac, A. *J. Am. Chem. Soc.* **2002**, *124*, 1698–1703.

(34) Huston, P.; Espenson, J. H.; Bakac, A. *J. Am. Chem. Soc.* **1992**, *114*, 9510–9516.

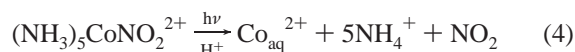
(35) Connolly, P.; Espenson, J. H.; Bakac, A. *Inorg. Chem.* **1986**, *25*, 2169–2175.

(36) Espenson, J. H. *Chemical Kinetics and Reaction Mechanisms*, 2nd ed.; McGraw-Hill: New York, 1995.

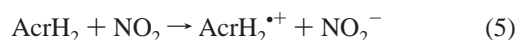
Steady-state photolysis was performed with the use of a Sperti Del Sol sunlamp, $\lambda_{\text{exc}} = 366 \text{ nm}$ ($\sim 75\%$) and 313 nm ($\sim 25\%$) at ambient temperature and pH 1.

Results

Reactions of NO_2 with AcrH_2 and with TMPD. The reaction between $0.7\text{--}2.45 \text{ mM}$ AcrH_2 and $2\text{--}10 \mu\text{M}$ NO_2 , generated by photolysis of 1.90 mM $(\text{NH}_3)_5\text{CoNO}_2^{2+}$ (dye laser) at pH 1, eq 4, followed biphasic kinetics at 640 nm where AcrH_2^{*+} is the only absorbing species. The kinetic traces consisted of a fast absorbance increase, followed by a slower return to the initial value.

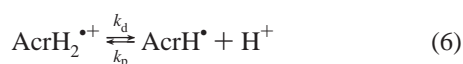


The use of higher concentrations of AcrH_2 resulted in gradually better fits, possibly indicating a smaller degree of interference from NO_2 dimerization. The plot of k_{obs} versus $[\text{AcrH}_2]$ for the faster stage in 40% AN was linear and gave the rate constant for reaction 5, $k_{\text{A}}^{40} = (9.4 \pm 0.2) \times 10^6 \text{ M}^{-1} \text{ s}^{-1}$.



The low solubility of AcrH_2 in 20% AN presented a problem because the rates for the two stages became comparable, which in turn reduced the precision of the rate constants obtained by consecutive biphasic fitting of experimental traces. The most reliable set of data was obtained by varying $[(\text{NH}_3)_5\text{CoNO}_2^{2+}]$, and thus $[\text{NO}_2]$, at a constant high $[\text{AcrH}_2]$ (0.35 mM). The bimolecular rate constant for the faster stage, $k_{\text{A}}^{20} = 2.2 \times 10^7 \text{ M}^{-1} \text{ s}^{-1}$, was obtained by extrapolation to $[(\text{NH}_3)_5\text{CoNO}_2^{2+}] = 0$, where the NO_2 self-reaction does not contribute.

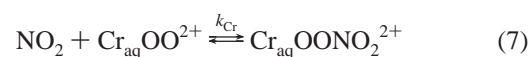
The rate constant for the slower stage, corresponding to the deprotonation of AcrH_2^{*+} , eq 6, remained unchanged under all conditions, $k_{\text{d}}^{20} = 2.5 \times 10^3 \text{ s}^{-1}$ and $k_{\text{d}}^{40} = 3.4 \times 10^3 \text{ s}^{-1}$. We associate an estimated standard error of 10% with these values.



The oxidation of $0.38\text{--}1.15 \text{ mM}$ TMPD with photogenerated NO_2 (Nd:YAG laser) was followed at 565 nm in 40% aqueous AN buffered with 0.05 M $\text{CH}_3\text{COOH}/0.05 \text{ M}$ CH_3COONa (pH 5.51). This reaction again proceeded in two stages, both exhibiting an absorbance increase. The [TMPD]-dependent phase yielded $k_{\text{T}}^{40} = (1.84 \pm 0.03) \times 10^8 \text{ M}^{-1} \text{ s}^{-1}$ and had an absorbance change that was 6–7 times larger than the absorbance change in the [TMPD]-independent step which had $k = 1.3 \times 10^4 \text{ s}^{-1}$. The overall absorbance changes showed a mild increase with the concentration of TMPD and reached a plateau at $[\text{TMPD}] \geq 1.2 \text{ mM}$. From this limit, the concentration of photogenerated NO_2 was calculated to be $[\text{NO}_2]_0 \sim 10 \mu\text{M}$.

The reaction between NO_2 and $\text{Cr}_{\text{aq}}\text{OO}^{2+}$ was monitored at 293 nm (Nd:YAG laser), where the absorbance decreased exponentially, yielding final absorbance readings that were stable for up to 10 ms. The pseudo-first-order rate constants were proportional to $[\text{Cr}_{\text{aq}}\text{OO}^{2+}]$ and yielded $k_{\text{Cr}}^{20} = (2.8 \pm 0.2) \times 10^8 \text{ M}^{-1} \text{ s}^{-1}$ and $k_{\text{Cr}}^{40} = (2.6 \pm 0.5) \times 10^8 \text{ M}^{-1} \text{ s}^{-1}$. The large errors in this analysis stem from a combination of small absorbance changes ($0.02\text{--}0.03$) and the large background absorbance.

Next, the photogenerated NO_2 was allowed to react with a mixture of $0.35\text{--}2.45 \text{ mM}$ AcrH_2 and 0.10 mM $\text{Cr}_{\text{aq}}\text{OO}^{2+}$ in 40% aqueous AN. The amount of AcrH_2 oxidized by NO_2 was determined from the absorbance changes at 640 nm . The total amount of AcrH^+ increased with the concentration of AcrH_2 in a nonlinear fashion, consistent with the competition between reactions in eqs 5 and 7.



The experimental data were fitted to eq 8, where $[\text{NO}_2]_0$ represents the concentration of NO_2 immediately after the flash. The fitting yielded $k_{\text{A}}/k_{\text{Cr}} = 0.032 \pm 0.004$, in close agreement with the ratio of the rate constants obtained by direct measurement, $k_{\text{A}}^{40}/k_{\text{Cr}}^{40} = 0.036 \pm 0.007$.

$$[\text{AcrH}^+]_{\infty} = [\text{NO}_2]_0 \frac{\frac{k_{\text{A}}[\text{AcrH}_2]}{k_{\text{Cr}}[\text{Cr}_{\text{aq}}\text{OO}^{2+}]}}{\frac{k_{\text{A}}[\text{AcrH}_2]}{k_{\text{Cr}}[\text{Cr}_{\text{aq}}\text{OO}^{2+}]} + 1} \quad (8)$$

Homolytic Cleavage of the $\text{Cr}_{\text{aq}}\text{OO}^{2+}/\text{NO}_2$ Adduct. The reaction between $45\text{--}194 \mu\text{M}$ $\text{Cr}_{\text{aq}}\text{OO}^{2+}$ and $10 \mu\text{M}$ NO_2 (dye laser) in the presence of $70\text{--}367 \mu\text{M}$ AcrH_2 was accompanied by a slow ($0.1\text{--}1 \text{ s}$) absorbance increase at 417 nm signaling the formation of AcrH^+ , Figure 1. This was followed by a much slower (seconds) linear increase in absorbance, which was shown to be caused by slow photolysis of $(\text{NH}_3)_5\text{CoNO}_2^{2+}$ with the analyzing light. This process was suppressed but not completely eliminated with the use of cutoff filters. The kinetic traces were fitted to an equation for parallel linear + exponential growth in absorbance.

Under the experimental conditions, the majority of NO_2 was initially captured by $\text{Cr}_{\text{aq}}\text{OO}^{2+}$ in $\ll 1 \text{ ms}$, as determined in experiments at 290 nm . The amount of AcrH^+ produced in the exponential portion of the trace at 417 nm was identical to the amount of NO_2 that had been captured by $\text{Cr}_{\text{aq}}\text{OO}^{2+}$ at submillisecond times. We interpret the process occurring in $0.1\text{--}1 \text{ s}$ as homolysis of $\text{Cr}_{\text{aq}}\text{OONO}_2^{2+}$ to regenerate NO_2 , eq 7, followed by the reaction between NO_2 and AcrH_2 , Scheme 1, where the oxidant (Ox) in eq 9 is either O_2 or $(\text{NH}_3)_5\text{CoNO}_2^{2+}$.

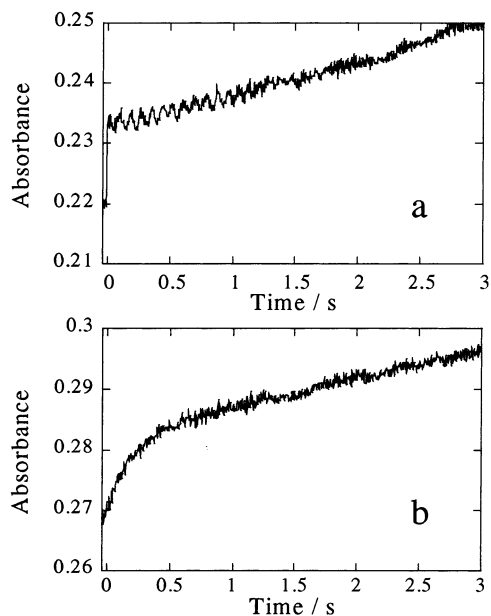
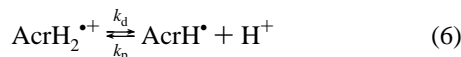
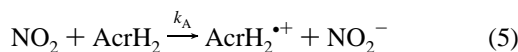


Figure 1. Absorbance increase at 417 nm caused by the growth of AcrH⁺ in the AcrH₂/NO₂ reaction at ambient temperature in aerated 20% aqueous acetonitrile, pH 1. (a) Reaction between AcrH₂ (70 μM) and NO₂ generated by laser flash photolysis (dye laser) of 1.8 mM (NH₃)₅CoNO₂²⁺. (b) 0.11 mM Cr_{aq}OO²⁺ added to reaction mixture in part a. In part b, the rapid initial formation of Cr_{aq}OONO₂²⁺ is followed by its homolysis to NO₂ and the reaction with AcrH₂. The slow, linear absorbance increase in both parts a and b is caused by photolysis with the analyzing light.

Scheme 1



At higher AcrH₂ concentrations, some NO₂ was captured initially by AcrH₂ in competition with Cr_{aq}OO²⁺, resulting in an initial absorbance jump. The overall absorbance changes remained constant, however, and matched those expected for a reaction between NO₂ and AcrH₂ in the absence of Cr_{aq}OO²⁺.

The observed homolysis rate was proportional to [AcrH₂] and inversely proportional to [Cr_{aq}OO²⁺]. By treating Cr_{aq}OONO₂²⁺ as a steady-state intermediate in Scheme 1, one obtains the rate law of eq 10, which can be rearranged to eq 11, where $k_{\text{H}}^{\text{obs}}$ represents the observed first-order rate constant and k_{H} is the rate constant for the homolysis of NO₂.

$$\text{rate} = k_{\text{H}} \frac{k_{\text{A}}[\text{AcrH}_2]}{k_{\text{A}}[\text{AcrH}_2] + k_{\text{Cr}}[\text{Cr}_{\text{aq}}\text{OO}^{2+}]} [\text{Cr}_{\text{aq}}\text{OONO}_2^{2+}] \quad (10)$$

$$k_{\text{H}}^{\text{obs}} = k_{\text{H}} \frac{1}{1 + \frac{k_{\text{Cr}}[\text{Cr}_{\text{aq}}\text{OO}^{2+}]}{k_{\text{A}}[\text{AcrH}_2]}} \quad (11)$$

Excellent fits of the experimental data to eq 11 were obtained, Figure 2, and yielded $k_{\text{H}}^{20} = 172 \pm 4 \text{ s}^{-1}$ and

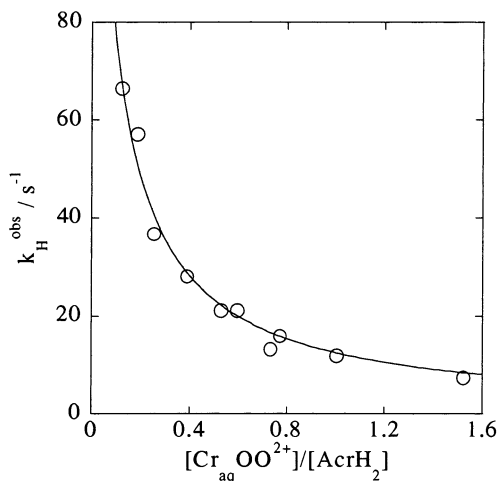


Figure 2. Plot of observed first-order rate constants $k_{\text{H}}^{\text{obs}}$ against $[\text{Cr}_{\text{aq}}\text{OO}^{2+}]/[\text{AcrH}_2]$ for the homolysis of Cr_{aq}OONO₂²⁺ produced in the reaction between Cr_{aq}OO²⁺ and NO₂, in the presence of AcrH₂. NO₂ was generated by laser flash photolysis (dye laser) of 2 mM (NH₃)₅CoNO₂²⁺ at ambient temperature in aerated 20% aqueous acetonitrile, pH 1. Solid line represents a fit to eq 11.

Table 1. Product Analysis Data for Steady State Photolysis^a of Cr_{aq}OO²⁺ and (NH₃)₅CoNO₂²⁺

[reactants]/μM		[products]/μM		
Cr _{aq} OO ²⁺	(NH ₃) ₅ CoNO ₂ ²⁺	NO ₂ ⁻	NO ₃ ⁻	Cr _{aq} OO ²⁺
260	0	0	0	235
0	210	84	84	0
260	210	63	103 ^b	180
108 ^c	300	<i>d</i>	<i>d</i>	81

^a Photolysis time: 45 s. ^b [NO₃⁻] + [Cr_{aq}OONO₂²⁺]. ^c Photolysis time: 80 s. ^d Not determined.

$k_{\text{H}}^{40} = 197 \pm 7 \text{ s}^{-1}$, although a realistic standard error is ~20%, i.e., comparable to that for k_{Cr} .

Product Analysis for the Cr_{aq}OO²⁺/NO₂ Reaction. Steady-state photolysis of 0.10–0.26 mM Cr_{aq}OO²⁺ and 0.21–0.30 mM (NH₃)₅CoNO₂²⁺ was carried out until all of the nitrocobalt complex was consumed, as determined from the UV–vis spectrum. Since Cr_{aq}OO²⁺ does not absorb significantly at the excitation wavelengths, the time of photolysis required for (NH₃)₅CoNO₂²⁺ alone and for the Cr_{aq}OO²⁺/(NH₃)₅CoNO₂²⁺ mixtures was chosen to be the same. Nitrate and nitrite ion concentrations were determined immediately after the photolysis. The amount of remaining Cr_{aq}OO²⁺ was determined from the absorbance at 293 nm after correction for the products of nitrocobalt photolysis. The results are summarized in Table 1.

Continuous photolysis of (NH₃)₅CoNO₂²⁺ (210 μM) gave 84 μM NO₂⁻ and 84 μM NO₃⁻, i.e., 40% of each based on the initial concentration of the cobalt complex. This result agrees precisely with the known photochemistry of (NH₃)₅CoNO₂²⁺.³⁷ Under our conditions, 80% should produce NO₂ followed by reaction 2, and 20% should isomerize to the photochemically inactive nitrito form. In the presence of Cr_{aq}OO²⁺, lower yields of NO₂⁻ (63 μM, 30%) and higher yields of nitrate³⁸ (103 μM, 49%) were observed, Table 1,

(37) Balzani, V.; Ballardini, R.; Sabbatini, N.; Moggi, L. *Inorg. Chem.* **1968**, *7*, 1398–1404.

third entry. This was accompanied by the consumption of some $\text{Cr}_{\text{aq}}\text{OO}^{2+}$ ($80 \mu\text{M}$), corresponding to about one-half of the amount of NO_2 generated by photolysis. When the concentration of the cobalt complex was raised, and that of $\text{Cr}_{\text{aq}}\text{OO}^{2+}$ lowered, $27 \mu\text{M}$ $\text{Cr}_{\text{aq}}\text{OO}^{2+}$ was consumed, Table 1, fourth entry. This amount is only $1/10$ of the total NO_2 produced. The closer inspection of the data shows that the $\text{Cr}_{\text{aq}}\text{OO}^{2+}$ consumed during photolysis corresponds to 25–30% of total $[\text{Cr}_{\text{aq}}\text{OO}^{2+}]$, independent of the absolute concentrations of the chromium and cobalt complexes used. Clearly, the reaction between $\text{Cr}_{\text{aq}}\text{OO}^{2+}$ and NO_2 under these conditions does not consume significant amounts of $\text{Cr}_{\text{aq}}\text{OO}^{2+}$ or generate new products. Most of the missing $\text{Cr}_{\text{aq}}\text{OO}^{2+}$ is accounted for by direct photolysis (10%), Table 1, first entry, and the reaction with HNO_2 produced in eq 2 (10–15%).

The lack of permanent products in the $\text{Cr}_{\text{aq}}\text{OO}^{2+}/\text{NO}_2$ reaction fully supports our conclusions reached in laser flash photolysis experiments which identified the homolysis of $\text{Cr}_{\text{aq}}\text{OONO}_2^{2+}$ as the main path for its disappearance, and the self-reaction of NO_2 as the main source of nitrogen-containing products.

Spectrum of $\text{Cr}_{\text{aq}}\text{OONO}_2^{2+}$. Two sets of experiments were carried out in 40% AN. The first set consisted of a series of laser flash photolysis (Nd:YAG) runs. The absorbance changes between the “zero” time (pretrigger value) and 5 ms after the laser flash, $\Delta\text{Abs}_{(\text{Co}+\text{Cr})}$, were recorded in the 280–330 nm range for a mixture of $\text{Cr}_{\text{aq}}\text{OO}^{2+}$ (0.1 mM) and $(\text{NH}_3)_5\text{CoNO}_2^{2+}$ (0.24 mM). The absorbance changes for $(\text{NH}_3)_5\text{CoNO}_2^{2+}$ alone, $\Delta\text{Abs}_{\text{Co}}$, were recorded in a control experiment. The 5-ms time difference ensures that all of the NO_2 had been converted to $\text{Cr}_{\text{aq}}\text{OONO}_2^{2+}$ at the point when the spectrum was recorded. Since NO_2 dimerization and hydrolysis make no significant contribution toward absorbance change in this wavelength range, the quantity $\Delta\text{Abs}_{\text{CrOO}/\text{NO}_2} = (\Delta\text{Abs}_{(\text{Co}+\text{Cr})} - \Delta\text{Abs}_{\text{Co}})$ corresponds to the absorbance change in the reaction between NO_2 and $\text{Cr}_{\text{aq}}\text{OO}^{2+}$, eq 12.

$$\Delta\text{Abs}_{\text{CrOO}/\text{NO}_2} = [\text{NO}_2]_0(\epsilon_{\text{CrOONO}_2} - \epsilon_{\text{CrOO}} - \epsilon_{\text{NO}_2}) \approx [\text{NO}_2]_0(\epsilon_{\text{CrOONO}_2} - \epsilon_{\text{CrOO}}) \quad (12)$$

It was confirmed with TMPD as a probe that the amount of NO_2 generated in a laser flash was reproducibly constant for a given concentration of $(\text{NH}_3)_5\text{CoNO}_2^{2+}$. This allowed us to compare directly the quantity $\Delta\text{Abs}_{\text{CrOO}/\text{NO}_2}$ with the absorbance changes calculated for the consumption of superoxochromium(III), $-\epsilon_{\text{CrOO}} \times [\text{NO}_2]_0$. The observed and calculated values were nearly the same, Figure 3, showing that $\epsilon_{\text{CrOONO}_2}$ is negligibly small throughout the spectral range examined.

The second set of experiments was based on the direct reaction between $\text{Cr}_{\text{aq}}\text{OO}^{2+}$ and N_2O_4 in the stopped-flow. An aqueous solution of 0.15 mM $\text{Cr}_{\text{aq}}\text{OO}^{2+}$ was mixed with 2–20 mM N_2O_4 in dry AN, and the temporal spectra were recorded in the 240–350 nm range. The only observed

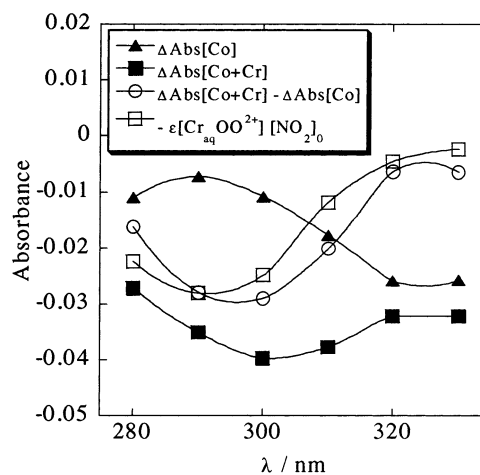


Figure 3. Absorbance changes recorded after laser flash photolysis (Nd:YAG laser) of 0.24 mM $(\text{NH}_3)_5\text{CoNO}_2^{2+}$ in the absence ($\Delta\text{Abs}_{\text{Co}}$) and in the presence of 0.10 mM $\text{Cr}_{\text{aq}}\text{OO}^{2+}$ ($\Delta\text{Abs}_{\text{Co}+\text{Cr}}$). Conditions: 40% aqueous acetonitrile, ambient temperature, pH 1. The difference $\Delta\text{Abs}_{\text{Co}+\text{Cr}} - \Delta\text{Abs}_{\text{Co}}$ is the absorbance change in the $\text{Cr}_{\text{aq}}\text{OO}^{2+}/\text{NO}_2$ reaction. The absorbance changes accompanying the consumption of $\text{Cr}_{\text{aq}}\text{OO}^{2+}$ are denoted as $-\epsilon_{\text{CrOO}} \times [\text{NO}_2]_0$.

absorbance changes were those associated with the loss of $\text{Cr}_{\text{aq}}\text{OO}^{2+}$, again showing that $\text{Cr}_{\text{aq}}\text{OONO}_2^{2+}$ does not absorb significantly in the 240–350 nm range.

Discussion

Reactions of Kinetic Probes. TMPD reacts with NO_2 to give $\text{TMPD}^{\bullet+}$ which was identified by its characteristic spectrum in the 500–700 nm region.³⁹ The rate constant obtained for this reaction is comparable to those for related reactions of NO_2 with substituted anilines, such as *N,N,N',N'*-tetramethylbenzidine, $k = 2.5 \times 10^8 \text{ M}^{-1} \text{ s}^{-1}$,⁴⁰ and 1,4-phenylenediamine, $k = 4.6 \times 10^7 \text{ M}^{-1} \text{ s}^{-1}$.⁴¹

One possible mechanism for the NO_2/TMPD reaction involves electron transfer from $\text{TMPD}/\text{TMPDH}^+$ ($\text{p}K_{\text{a}} = 5.79$, see Experimental Section) to NO_2 , followed by deprotonation of the radical dication TMPDH^{2+} , eqs 13–14, a process known to proceed with positive absorbance changes in the 500–700 nm range.³⁹



If the reaction indeed takes place by electron transfer, then the $[\text{TMPD}]$ -independent step represents the deprotonation of TMPDH^{2+} . The absorbance changes in this step translate into significant concentrations of TMPDH^{2+} , showing that a measurable portion of NO_2 had reacted with TMPDH^+ in competition with TMPD. The pH of the acetate buffer (pH 5.51) is lower than the $\text{p}K_{\text{a}}$ of TMPDH^+ by only 0.28 pH units so that the two forms of TMPD exist at comparable concentrations, 34% TMPD and 66% TMPDH^+ . Thus, the rate constants of electron transfer from TMPD and TMPDH^+

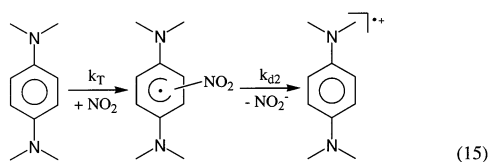
(38) Some of the nitrate was present as $\text{Cr}_{\text{aq}}\text{ONO}_2^{2+}$, a chromium–nitrate complex produced in a thermal reaction between $\text{Cr}_{\text{aq}}\text{OO}^{2+}$ and HNO_2 , ref 27.

(39) Rao, P. S.; Hayon, E. *J. Phys. Chem.* **1975**, *79*, 1063–1066.

(40) Frank, A. J.; Graetzel, M. *Inorg. Chem.* **1982**, *21*, 3834–3837.

(41) Huie, R. E.; Neta, P. *J. Phys. Chem.* **1986**, *90*, 1193–1198.

would have to be comparable to explain our data. In view of the much greater reactivity of TMPD over TMPDH⁺ in other electron transfer reactions,^{42,43} we consider this unlikely and look for another mechanism, such as that in eq 15, whereby NO₂ first adds to the aromatic ring, followed by the release of NO₂⁻.



Similar chemistry has been reported for the oxidation of TMPD with OH radicals,³⁹ where the sign and magnitude of absorbance changes for the dissociation of OH⁻ from an initially formed adduct are similar to those observed in this study. The rate constant k_{d2} is also comparable to that for OH⁻ dissociation from the OH adduct, $(8-10) \times 10^4 \text{ s}^{-1}$. Since TMPD was used in this study only as a kinetic probe, further investigation of this chemistry was not carried out.

In the reaction between NO₂ and AcrH₂, the build-up of the characteristic absorption at 640 nm suggests an electron transfer mechanism yielding AcrH₂^{•+},³² a transient that undergoes deprotonation and further oxidation to AcrH⁺, Scheme 1. This mechanism is accompanied by a significant charge separation in the transition state and is supported by the observed lowering of the rate constant k_A (see Scheme 1) as the polarity of the solvent decreases by an increase in AN content from 20% to 40%.

An alternative path, the addition of NO₂ to one of the aromatic rings of AcrH₂ followed by the release of HNO₂ and oxidation to the final product, would entail a partial loss of aromaticity in AcrH₂ and is apparently disfavored. It is not clear, however, why the loss of aromaticity should be more restricting with AcrH₂ than with TMPD, which appears to react by NO₂ addition.

The AcrH[•] radical is strongly reducing, $E^0(\text{AcrH}^+/\text{AcrH}^\bullet) = -0.19 \text{ V}$ versus NHE, and its oxidation is often diffusion-controlled.⁴⁴ It is reasonable to assume that either molecular oxygen or (NH₃)₅CoNO₂²⁺, both present at millimolar levels in our solutions, are capable of rapidly oxidizing AcrH[•], as shown in eq 9, Scheme 1. Under these conditions, the deprotonation of AcrH₂^{•+} becomes rate limiting. Consecutive biexponential fits of kinetic traces at 640 nm yielded $k_d^{20} = 2.5 \times 10^3 \text{ s}^{-1}$ in 20% AN and $k_d^{40} = 3.4 \times 10^3 \text{ s}^{-1}$ in 40% AN. These figures are close to the indirectly determined value of 690 s^{-1} (20% acetonitrile),³² which is based on an estimated diffusion-controlled rate constant for the reaction between AcrH[•] and Ce_{aq}⁴⁺.

AcrH₂, which is often used as a model for NADH, is much more reactive toward NO₂ than NADH itself. The upper limit for the rate constant for the NADH reaction is $2 \times 10^5 \text{ M}^{-1} \text{ s}^{-1}$, and the true value is probably no larger than 10^3 M^{-1}

Table 2. Summary of Rate Constants at 25 °C Determined in This Study

reaction	k^a	
	20% AN	40% AN
(1) AcrH ₂ + NO ₂ → AcrH ₂ ^{•+} + NO ₂ ⁻	2.2×10^7	$(9.4 \pm 0.2) \times 10^6$
(2) AcrH ₂ ^{•+} → AcrH [•] + H ⁺	2.5×10^3	3.4×10^3
(3) NO ₂ + TMPD → NO ₂ -TMPD [•]	690^b	$(1.84 \pm 0.03) \times 10^8$
(4) NO ₂ -TMPD [•] → NO ₂ ⁻ + TMPD ^{•+}		1.3×10^4
(5) NO ₂ + Cr _{aq} OO ²⁺ → Cr _{aq} OONO ₂ ²⁺	$(2.8 \pm 0.2) \times 10^8$	$(2.6 \pm 0.5) \times 10^8$
(6) Cr _{aq} OONO ₂ ²⁺ → NO ₂ + Cr _{aq} OO ²⁺	172 ± 4	197 ± 7

^a Units: M⁻¹ s⁻¹ for reactions 1, 3, and 5; s⁻¹ for reactions 2, 4, and 6. ^b Ref. 32.

s⁻¹,⁴⁵ i.e., several orders of magnitude lower than k_A determined in this study for AcrH₂. This result can be rationalized on the basis of thermodynamics. The one-electron reduction potentials of AcrH₂^{•+}/AcrH₂ and NADH^{•+}/NADH couples are 0.70 and 1.02 V, respectively,^{32,46} and that for NO₂/NO₂⁻ is 1.04 V.⁴⁷ Thus, the NADH/NO₂ reaction is approximately thermoneutral, while the AcrH₂/NO₂ reaction has a driving force of +0.34 V. Further analysis by Marcus cross relation and using $k_{\text{self}} = 10^{-0.5}$ for NO₂/NO₂⁻⁴⁸ and $\sim 10^9$ for AcrH₂^{•+}/AcrH₂ (an estimate for a large organic molecule with delocalized electron density) affords $\log k_A \sim 7$, a result that is in excellent agreement with experimental data.}}}

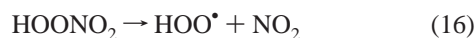
The NO₂/Cr_{aq}OO²⁺ Reaction. When Cr_{aq}OO²⁺ was introduced into the AcrH₂/(NH₃)₅CoNO₂²⁺ system, the amount of AcrH₂^{•+} produced in the rapid (millisecond) AcrH₂/NO₂ reaction decreased as the concentration of Cr_{aq}OO²⁺ increased. The direct kinetic determination of the Cr_{aq}OO²⁺/NO₂ reaction at 290 nm in conjunction with the analysis of the kinetic product ratio at 640 nm was consistent with a simple competition between AcrH₂ and Cr_{aq}OO²⁺ for NO₂. Unlike the AcrH₂/NO₂ case, the solvent polarity had a negligible effect on the rate constant for the Cr_{aq}OO²⁺/NO₂ reaction or its reverse, see Table 2. This observation, as well as the magnitude of the Cr_{aq}OO²⁺/NO₂ rate constant, can be readily explained if one views this reaction as a radical coupling process, as shown in eq 7. There is very little charge separation or build-up in the transition state for such a reaction, rendering any solvent polarity effects on rates minimal.

The rate constant for the reactions between Cr_{aq}OO²⁺ and NO₂ ($k_{\text{Cr}} = 2.8 \times 10^8 \text{ M}^{-1} \text{ s}^{-1}$) is only an order of magnitude smaller than that for the reaction between HO₂[•] and NO₂ ($k = 1.8 \times 10^9 \text{ M}^{-1} \text{ s}^{-1}$).⁴⁹ A difference of this magnitude can be easily explained by the binding of the superoxide to a metal center. In another example of such a deceleration, the rate constant for the Cr_{aq}OO²⁺/NO reaction²⁷ is approximately 10 times smaller than that for the diffusion-controlled HO₂[•]/NO reaction.⁵⁰

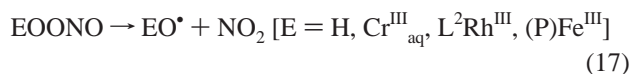
(42) Nickel, U.; Jaenicke, W. *Ber. Bunsen-Ges. Phys. Chem.* **1982**, *86*, 695–701.
 (43) Neta, P.; Huie, R. E. *J. Phys. Chem.* **1985**, *89*, 1783–1787.
 (44) Fukuzumi, S.; Tokuda, Y.; Kitano, T.; Okamoto, T.; Otera, J. *J. Am. Chem. Soc.* **1993**, *115*, 8960–8968.

(45) Goldstein, S.; Czapski, G. *Chem. Res. Toxicol.* **2000**, *13*, 736–741.
 (46) Matsue, T.; Suda, M.; Uchida, I.; Kato, T.; Akiba, U.; Osa, T. *J. Electroanal. Chem. Interfacial Electrochem.* **1987**, *234*, 163–173.
 (47) Ram, M. S.; Stanbury, D. M. *Inorg. Chem.* **1985**, *24*, 2954–2962.
 (48) Stanbury, D. M. *Adv. Chem. Ser.* **1997**, *253*, 165–182.
 (49) Loegager, T.; Sehested, K. *J. Phys. Chem.* **1993**, *97*, 10047–10052.

To the best of our knowledge, this work provides the first documented example of a direct interaction between NO₂ and a superoxometal complex. The reaction leads to the formation of a peroxy-nitrato metal complex. The O–N bond, formed in the process, is clearly weak and undergoes facile homolytic cleavage. The rate constant for this process, 172 s⁻¹ in 20% AN, is several orders of magnitude greater than that for the uncoordinated peroxy-nitric acid HOONO₂, for which the reported values of *k*₁₆, eq 16, range from 4.6 × 10⁻³ to 0.05 s⁻¹.^{51–53}



The large difference in homolysis rates between free peroxy-nitric acid and metal-bound peroxy-nitrato is similar to the observed differences in homolysis rate constants for the O–O bond cleavage in free peroxy-nitrous acid and metal peroxy-nitrites, eq 17.



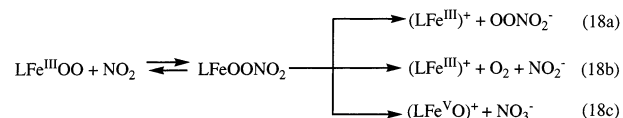
Again, the metal-bonded anion reacts much faster.^{33,54–56} Coordination to a metal center clearly weakens the bond, presumably because of the increased thermodynamic stability of the oxo–metal product relative to hydroxyl radicals.

The weak UV absorption spectrum of Cr_{aq}OONO₂²⁺ is as expected by comparison with the uncoordinated species. The peroxy-nitrato anion has a fairly strong UV absorption ($\epsilon_{285} = 1.65 \times 10^3 \text{ M}^{-1} \text{ cm}^{-1}$),⁴⁹ but the protonated form HOONO₂ exhibits only a weak maximum at 245 nm ($\epsilon = 400 \text{ M}^{-1} \text{ cm}^{-1}$).

On the basis of the findings in this work, it is tempting to suggest that other superoxometal complexes, including oxyhemoglobin and oxymyoglobin, may also react with NO₂ to yield transient peroxy-nitrato compounds. Such a proposal is additionally justified by the known reaction of NO with HbO₂ to form HbOONO,⁵⁵ showing that HbO₂ can indeed participate in radical coupling reactions.

The stability and ultimate fate of such putative peroxy-nitrato complexes need by no means follow that observed for Cr_{aq}OONO₂²⁺. In addition to homolysis of the N–O

bond, there are several other reasonable possibilities to be considered, as shown in eq 18.



Consistent with the path in eq 18a, the peroxy-nitrato anion was suggested as one of the possible intermediates generated from NO₂ and oxyhemoglobin⁵⁷ in the autocatalytic oxidation of hemoglobin by nitrite, but the metal-coordinated peroxy-nitrato was not considered.

The chemistry in eq 18b is thermodynamically favorable for oxyglobins,⁵⁸ although this path cannot explain the autocatalytic features of the nitrite reaction²⁸ if the NO₂/HbOO step is indeed involved, as proposed.^{24,28,57}

The process in eq 18c is reminiscent of a step proposed in the mechanism of action of cytochrome P450 enzymes,⁵⁹ whereby a hydroperoxoiron(III) complex is converted in an acid-catalyzed step to an oxene, formally an Fe(V) complex. A similar reaction has been observed directly with a macrocyclic hydroperoxochromium(III) complex.⁶⁰ In the present case, eq 18c, the catalysis by H⁺ is not required owing to the stability of the leaving anion NO₃⁻. Since the formation of higher oxidation states of iron heme complexes is not as energetically demanding as it is for aqua chromium complexes,⁶¹ a heterolytic cleavage of the O–O bond as in eq 18c cannot be ruled out, and it may be an important step in the poorly understood autocatalytic oxidation of hemoglobin by nitrite.

In addition to the potential decay paths described, the peroxy-nitrato metal complexes are also expected to act as oxidants toward other substrates. In our earlier study of the reaction between nitrous acid and a macrocyclic superoxorhodium(III) complex, L²RhOO²⁺ (L² = *meso*-Me₆-[14]-ane-N₄), we presented some evidence for a transient L²RhOONO₂²⁺ and its subsequent reaction with nitrous acid.⁶² Studies of the chemical properties and reactivity of peroxy-nitrato metal species are currently in progress in our laboratory.

Acknowledgment. This work was supported by a grant from the National Science Foundation, CHE 9982004. Some of the work was conducted with the use of facilities at the Ames Laboratory.

IC026315S

(50) Goldstein, S.; Czapski, G. *Free Radical Biol. Med.* **1995**, *19*, 505–510.

(51) Lammel, G.; Perner, D.; Warneck, P. *J. Phys. Chem.* **1990**, *94*, 6141–6144.

(52) Regimbal, J.-M.; Mozurkewich, M. *J. Phys. Chem. A* **1997**, *101*, 8822–8829.

(53) Goldstein, S.; Czapski, G. *Inorg. Chem.* **1997**, *36*, 4156–4162.

(54) Goldstein, S.; Czapski, G.; Lind, J.; Merenyi, G. *Chem. Res. Toxicol.* **2001**, *14*, 657–660.

(55) Herold, S. *FEBS Lett.* **1998**, *439*, 85–88.

(56) Lee, J.; Hunt, J. A.; Groves, J. T. *J. Am. Chem. Soc.* **1998**, *120*, 7493–7501.

(57) Doyle, M. P.; Herman, J. G.; Dykstra, R. L. *J. Free Radicals Biol. Med.* **1985**, *1*, 145–153.

(58) Sutton, H. C.; Sangster, D. F. *J. Chem. Soc., Faraday Trans. 1* **1982**, *78*, 695–711.

(59) Guengerich, F. P.; Macdonald, T. L. *Acc. Chem. Res.* **1984**, *17*, 9–16.

(60) Bakac, A.; Wang, W.-D. *J. Am. Chem. Soc.* **1996**, *118*, 10325–10326.

(61) Bakac, A. *Prog. Inorg. Chem.* **1995**, *43*, 267–351.

(62) Pestovsky, O.; Bakac, A. *Inorg. Chem.* **2002**, *41*, 901–905.